# Supplementary Information for

# Material properties of the cell dictate stress-induced spreading and differentiation in embryonic stem cells

Farhan Chowdhury, Sungsoo Na, Dong Li, Yeh-Chuin Poh, Tetsuya S. Tanaka, Fei Wang, Ning Wang*

* To whom correspondence should be addressed. E-mail: nwangrw@illinois.edu

**This PDF file includes ADDITIONAL METHODS and SUPPLEMENTARY FIGURES.**

## ADDITIONAL METHODS

**Variation of polyacrylamide gel substrate stiffness.** Polyacrylamide gels were made as described before[1,2]. The elastic Young's modulus of the polyacrylamide gels used in this study was 0.15 kPa (0.04% bis-acrylamide, 3% polyacrylamide), 0.6 kPa (0.06% bis-acrylamide, 3% polyacrylamide), 3.5 kPa (0.1% bis-acrylamide, 5% polyacrylamide) and 8 kPa (0.3% bis-acrylamide, 5% polyacrylamide)[3,4]. 0.2μm yellow-green fluorescent microspheres (Molecular Probe) were embedded onto the gels for traction measurements. In some experiments, prepared gels and rigid glass substrates were coated with type I collagen (100 μg/ml and 40 μg/ml respectively). In some experiments, rigid glass substrates were coated with low type I collagen concentration of 1 ng/ml to maintain the cell in a rounded shape.

**Applying a local stress using magnetic twisting cytometry.** Briefly, ferromagnetic microbeads (4 μm in diameter) were coated with ligands to integrin receptors (a synthetic peptide containing the Arg–Gly–Asp (RGD) sequence) or with poly-l-lysine (Sigma), both at 50 μg/ml per mg bead. The RGD-coated beads were incubated for 10-15 min to adhere to the apical surface of the cells so that they become tightly bound to the F-actin cytoskeleton via focal adhesions (Supplementary Fig. S11). The beads were magnetized horizontally using a strong (1000 gauss (G)) and short (<0.1ms) magnetic impulse. A twisting field was applied by a sinusoidally varying perpendicular magnetic field resulting in translational bead displacement induced by bead rotation. The bead movement was quantified using an intensity weighted center of mass algorithm. An inverted Leica microscope was used. A black and white charge-coupled device camera (Hamamatsu, C4742-95-12ERG) was attached to the camera side port of the microscope. Image acquisition was phase-locked with the sinusoidal twisting field. In our study, the magnetic twisting field was varied at 0.03, 0.3, 1, or 3 Hz. The amplitude of the oscillating field

was varied at 0, 10, or 50 G. The apparent applied stress defined as the ratio of the applied torque to six times the bead volume and equals the bead constant times the applied twisting field. The bead constant was calibrated in a viscosity standard and determined to be 0.35 Pa per G. Therefore, the applied stress was 0, 3.5, or 17.5 Pa corresponding to the above applied magnetic field respectively. In all our loading experiments, mES cells were plated in low serum medium (1%). However, we found that a local cyclic stress also induced cell spreading in mES cells in the absence of serum, although at longer times, the extent of spreading appeared to be somewhat less prominent in zero serum than in 1% serum (Supplementary Fig. S12).

**Cell softness quantification.** As defined in the previous Methods section, the cell complex softness is the ratio of strain to the applied stress (i.e., the applied specific torque) and thus is the inverse of the cell complex stiffness. Acquired bead displacements in response to the applied stress were stored for further analysis using a custom-made Matlab program. Bead displacements were displayed on an image window where one could select individual beads for analysis. The beads whose displacement waves conformed to the input sinusoidal signals at the same frequency were selected. This was necessary to filter out spontaneous movements of the beads or microscope stage shifts. Beads with displacements less than 5 nm (detection resolution) and loosely bound beads were not selected for analysis. To increase the signal to noise ratio, the peak amplitude of the displacement "d" (nm) was averaged over 5 consecutive cycles. The complex stiffness is measured by applying an oscillatory magnetic field and measuring the resultant oscillatory bead motions using the relation G*=T/d. For each bead, the elastic stiffness *G'* (the real part of G*) and the dissipative stiffness *G"* (the imaginary part of G*) was calculated based on the phase lag. The measured stiffness has the units of torque per unit bead volume per unit bead displacement (Pa/nm), which is model-free. In our cells the bead was

embedded ~50% into the cell surface (Supplementary Fig. S13), similar to those found in other cell types in a recent report[5]. If one uses a 50% bead-cell surface contact area and an established finite element model to convert stiffness (Pa/nm) to modulus (Pa)[6], then 1 Pa/nm stiffness is equivalent to 2.5 kPa modulus. Cell softness values were obtained by taking the inverse of the cell modulus values and have the unit of $kPa^{-1}$.

**Cell area and traction measurements**. Briefly, a displacement field was calculated by comparing a fluorescent submicron bead image at a particular time point during the experiment with a reference image captured at the end of the experiment by trypsinizing the cell from its underlying substrates. Knowing the substrate rigidity and the displacement field, a traction field was computed by solving this inverse problem.

**Lentivirus production and mES cell infection**. Briefly, HEK293T cells were purchased from American Type Culture Collection (ATCC) and were cultured according to ATCC recommendations. HEK293T cells were plated for 24 hrs before transfection. After reaching 70-80% confluency, cells were transfected with target or non-target shRNA control plasmids using the Fugene 6 reagent (Roche). The medium was replaced after overnight incubation of cells, with the virus packaging medium containing DMEM, 30% FBS, 1 mM sodium pyruvate, 4mM glutamine. Supernatant containing the lentivirus was collected 48-72 h later.

To infect mES cells, lentiviruses were mixed with mES cells culture medium, and the mixture was incubated with 0.25% Trypsin-EDTA digested mES cells for 12 h. 6 μg/mL Polybrene (Sigma) was used to improve the efficiency of infection. Virus-containing medium was changed with fresh culture medium. After 5 d, the cells were harvested for additional assay.

**Drugs, antibodies, and immunofluorescence staining.** LatA, PDGF, Rhodamine-phalloidin, Hoechst 33342 were from Sigma. Blebbistatin was from Toronto Research Chemicals. PP1 and

ML-7 were from Biomol. NSC23766 was from Tocris Bioscience. Y-27632 was from Calbiochem. Anti phospho-MLC antibodies (Thr18/ Ser19, IF 1:50) and Cdc42 antibodies (WB 1:1000) were from Cell Signaling Technology. Goat anti-GAPDH (HRP) polyclonal antibody (WB 1:10,000) from Genscript Corporation and secondary antibodies (IF 1:100 and 1:200, WB 1:10,000) were from Abcam. For immunofluorescence microscopy, cells were fixed with 4% paraformaldehyde and permeabilized with 0.5% Triton X-100. Cells were incubated with primary antibodies at 4 °C overnight and secondary antibody labeling was performed at room temperature for 1 hr. The actin cytoskeleton was stained using 0.76 μM Rhodamine-phalloidin for 20 minutes. The DNA was counter-stained with 1-10 μg/ml Hoechst 33342 for 10 min and the coverslips were rinsed three times in cytoskeleton buffer solution and once in $dH_2O$ before mounting. F-actin content was quantified along the lines shown using ImageJ.

**References**


1. Pelham, R. J. Jr & Wang, Y. Cell locomotion and focal adhesions are regulated by substrate flexibility. *Proc. Natl. Acad. Sci. U.S.A.* **94**, 13661-13665 (1997).
2. Wang, N. et al. Cell prestress. I. Stiffness and prestress are closely associated in adherent contractile cells. *Am. J. Physiol. Cell Physiol.* **282**, C606-C616 (2002).
3. Yeung, T. et al. Effects of substrate stiffness on cell morphology, cytoskeletal structure, and adhesion. *Cell Motil. Cytoskeleton* **60**, 24-34 (2005).
4. Engler, A. et al. Substrate compliance versus ligand density in cell on gel responses. *Biophys. J.* **86**, 617-628 (2004).
5. Kasza, K. E. et al. Filamin A is essential for active cell stiffening but not passive stiffening under external force. *Biophys. J.* **96**, 4326-4335 (2009).

6. Mijailovich, S. M., Kojic, M., Zivkovic, M., Fabry,B. & Fredberg, J. J. A finite element model of cell deformation during magnetic bead twisting. *J. Appl. Physiol*. **93**, 1429-1436 (2002).

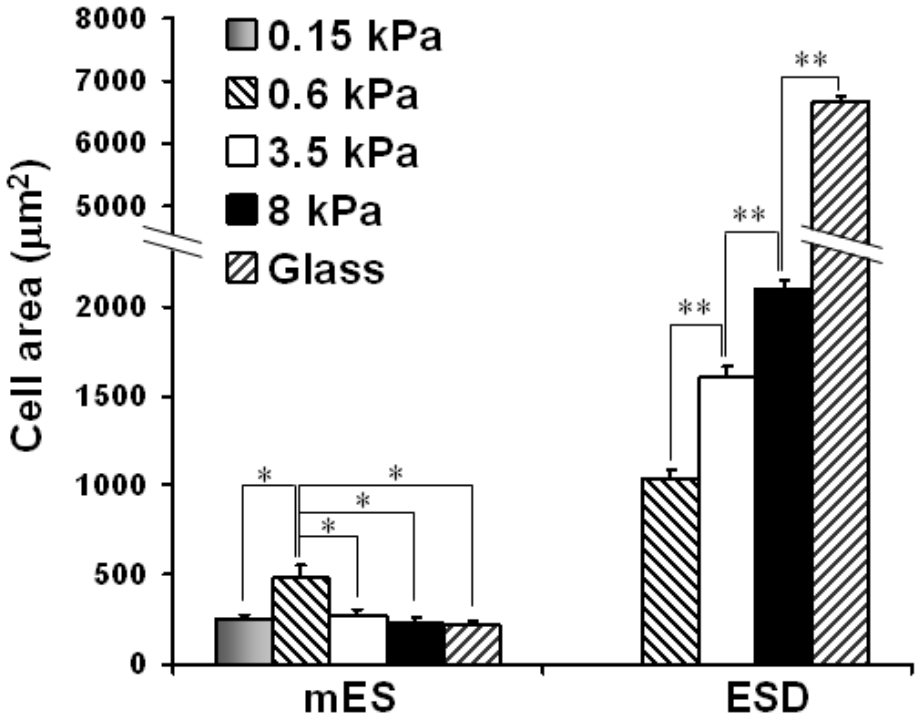


**Fig. S1.** Embryonic stem (ES) cells spread optimally on substrate of 0.6 kPa. Cells were plated overnight on collagen-1 coated substrates with rigidity of 0.15-kPa, 0.6-kPa, 3.5-kPa, or 8-kPa polyacrylamide gel, or rigid glass. *Left*: ES cells (n=9 cells for 0.15 kPa, 8 for 0.6 kPa, 7 for 3.5 kPa, 7 for 8 kPa, 12 for glass). *Right:* cells differentiated from ES cells (ESD) (n=12 cells for 0.6 kPa, 9 for 3.5 kPa, 8 for 8 kPa, 15 for glass). Means ± s.e.; at least three independent experiments. (* $p<0.05$; ** $p<0.001$).

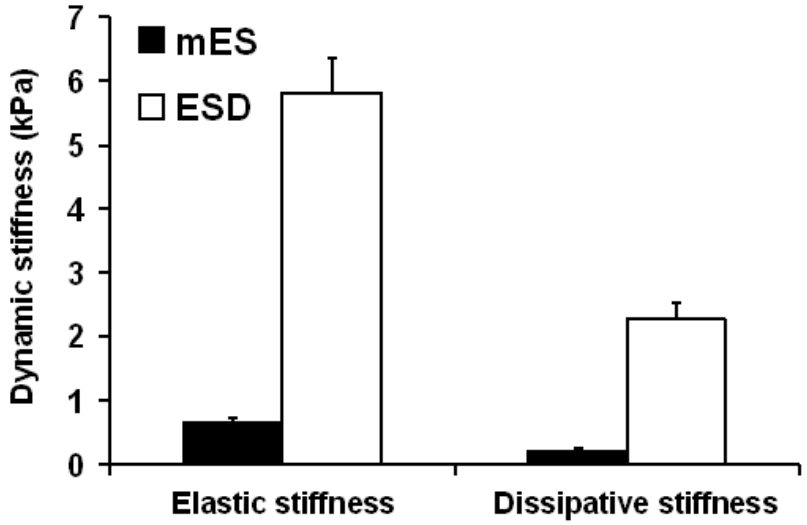


**Fig. S2.** mES cells are ~10-fold softer than their differentiated counterpart ESD cells. An oscillatory stress of 17.5 Pa at 0.3 Hz was applied to either ES cells or ESD cells via RGD-coated magnetic beads. Cells were plated overnight on collagen-1 (40 μg/ml) coated glass dishes. Although ES cells generally appear in lumps[48], their stiffness values do not change whether they are single individual cells or in lumps. In all our experiments, we chose to use only sparsely plated, single individual ES cells in order to precisely quantify cell area changes. The elastic stiffness or dissipative stiffness of the cells was computed[48]. n=~200 mES cells, and n=~250 ESD cells. At least 3 separate experiments (data replotted from ref. 48 in the main text).

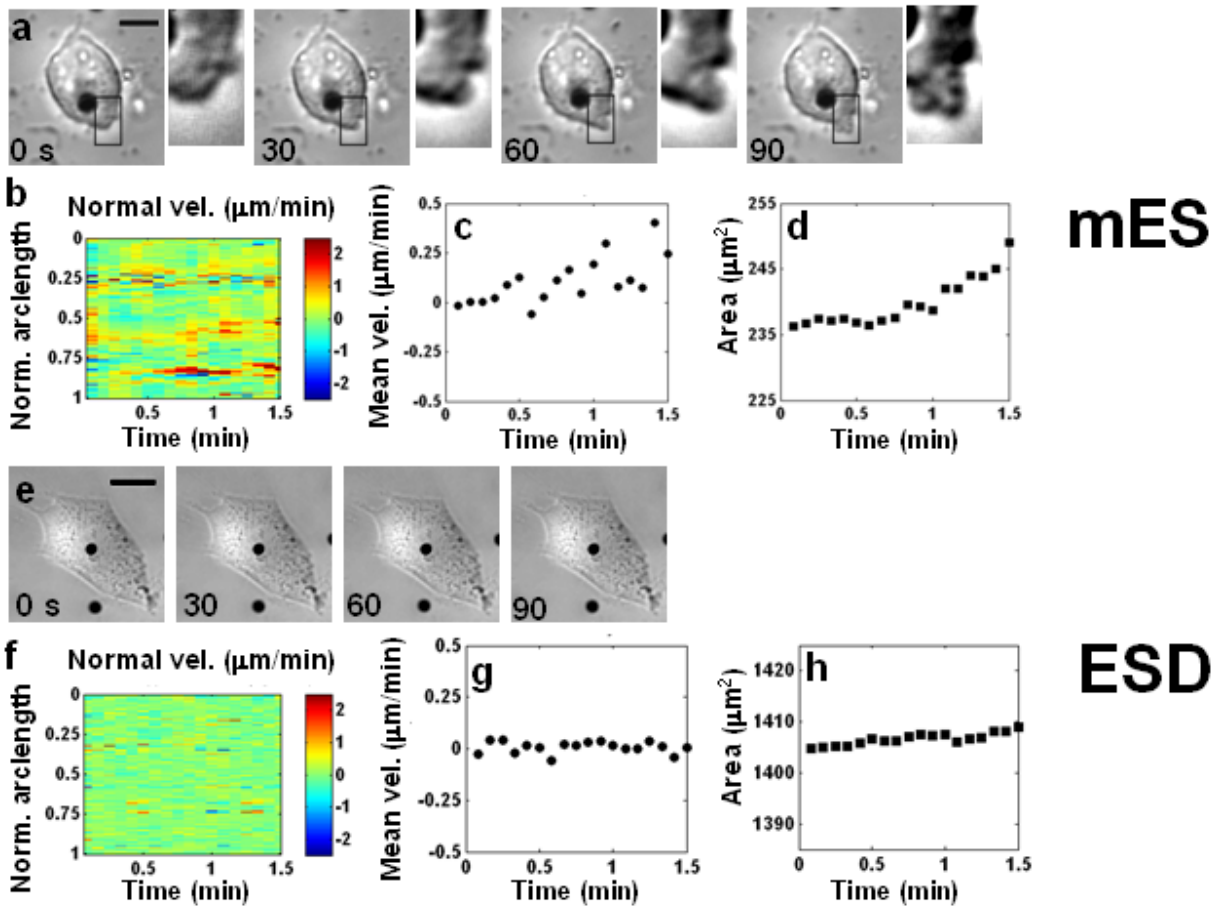


**Fig. S3.** A mouse embryonic stem (mES) cell (**a**-**d**) but not an embryonic stem cell-differentiated (ESD) cell (**e**-**h**) spreads in response to a local cyclic stress. A 4-μm RGD-coated ferromagnetic bead (the black dot) was attached to the apical surface of the cell for 15 min via integrins around. A local oscillatory stress of 17.5 Pa at 0.3 Hz was applied continuously. **a**, The applied stress induced a protrusion in an ES cell as early as 30 sec that grew with time (insets). (Scale bar, 10 μm.) **b**, Quantitative analyses of periphery movement velocity normal to the cell boundary in the ES cell (Normal vel; protrusion is shown as positive values; retraction is shown as negative values). The normal velocity is shown as a function of normalized arclength of the cell contour and time[24]. Note on the normal velocity map there are three visible "hotspot" bands

indicating the spreading of ES cells induced by mechanical stress. **c**, Mean normal velocity around the ES cell periphery is shown as a function of time. A greater than zero value represents an overall spreading of the cell induced by the stress. **d**, Progressive protrusions around the cell periphery resulted in an increase in cell area of the ES cell. **e**, The ESD cell failed to spread in response to the same amplitude of mechanical stress. (Scale bar, 20 μm.) **f**, Normal velocity map of cell periphery indicates that the ESD cell was relatively quiescent and unresponsive. **g**, Mean normal velocity of the ESD cells was zero over time, suggesting lack of response to the mechanical stress. **h**, No change in the projected area of the ESD cell was observed over time. In general, mES cells form colonies. mES cells in a colony also spread in response to a local cyclic stress (17.5 Pa at 0.3 Hz) (see Supplementary Fig. S14), suggesting that our findings on individual single cells are applicable to a colony of mES cells.

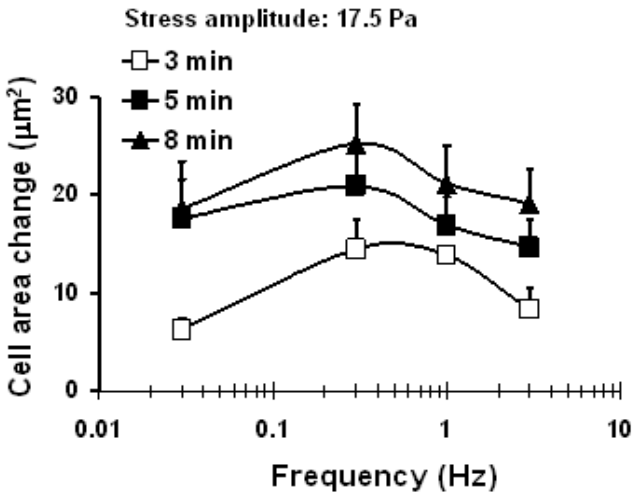


**Fig. S4.** Stress-induced early spreading in ES cells is stress frequency dependent. Stress amplitude was fixed at 17.5 Pa. Three minutes after loading, there were significant differences in cell area changes between 0.03 and 0.3 Hz ($p<0.01$) and between 1 and 3 Hz ($p<0.03$) but no difference between 0.3 and 1 Hz ($p>0.48$). At later times after onset of loading (5 and 8 min), there were no differences in cell areas between different frequencies. In contrast to 3 min loading in which loading frequency is optimal at 0.3-1 Hz, at 5 min loading, there were no significant differences: $p>0.20$ between 0.03 and 0.3 Hz; $p>0.09$ between 0.3 and 1 Hz; $p>0.59$ between 1 and 3 Hz respectively. At 8 min, there were no significant differences: $p>0.10$ between 0.03 and 0.3 Hz; $p>0.15$ between 0.3 and 1 Hz; $p>0.69$ between 1 and 3 Hz respectively. n=6, 9, 8, or 9 cells at 0.03, 0.3, 1, or 3 Hz respectively (three separate experiments).

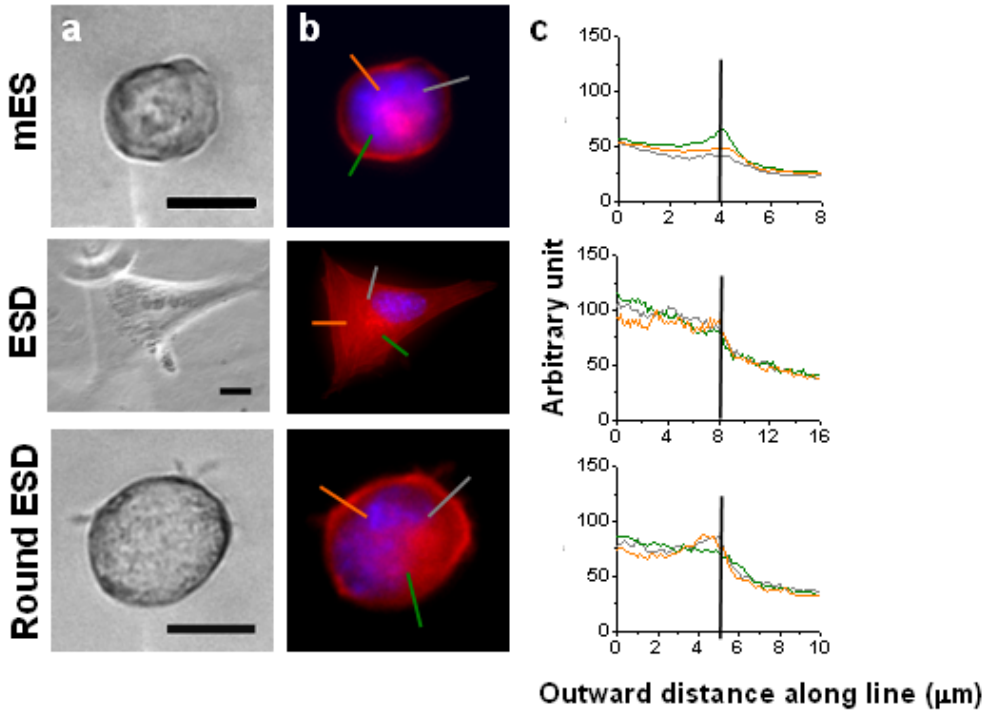


**Fig. S5**. F-actin distribution in mES cells, ESD cells, and round ESD cells on low matrix proteins (1 ng/ml collagen-1). **a**, Phase contrast images of representative mES, ESD, or round ESD cell. **b**, Cells were stained with rhodamin-phalloidin for F-actin (red) and Hoechst 33342 for DNA (blue). Three color lines were arbitrarily selected for quantifying F-actin fluorescent intensity at 3 different cytoplasm regions. **c**, F-actin fluorescent intensities along the 3 color lines in each cell. The F-actin densities are lowest in the mES cell, medium in the round ESD cell, and highest in the spread ESD cell. The F-actin densities appear to be inversely correlated with cell softness and consistent with the mechanical data of these cells in Fig. 1b. Solid vertical lines represent cell edges. (Scale bar, 15 μm.)

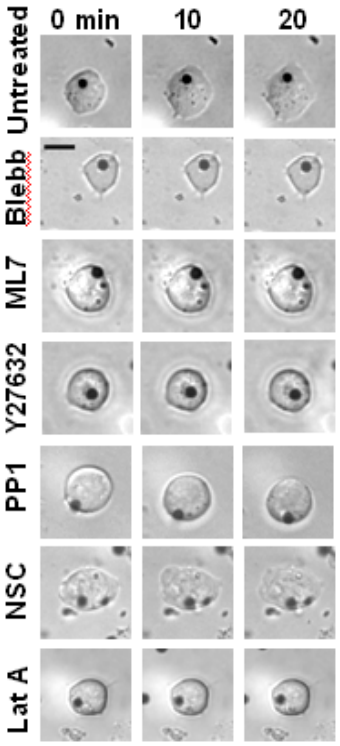


**Fig. S6.** Brightfield images of representative mES cells in response to stress after different drug treatments. Untreated: control cell; Blebb: Blebbistatin (50 μM for 30min) to inhibit myosin II ATPase; ML7 (25 μM for 20min) to inhibit myosin light chain kinase; Y27632 (50 μM for 20 min) to inhibit ROCK;, PP1 (10 μM for 1hr) to inhibit Src; NSC: NSC23766 (100 μM for 1 hr) to inhibit Rac; Lat A: Latrunculin A (0.1 μg/ml for 30 min) to disrupt actin microfilaments. Clearly stress-induced spreading in mES cells are dependent on myosin II, F-actin, ROCK and Src, but not on Rac activity. (Scale bar, 15 μm applies to all cells)

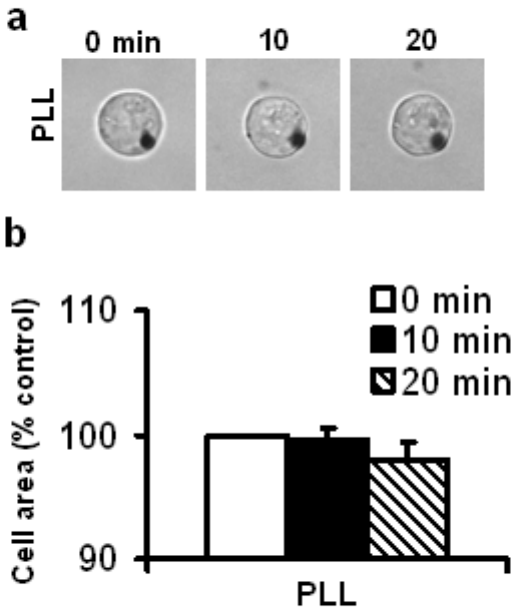


**Fig. S7.** Nonspecifically stressing mES cells with Poly-L-lysine coated beads did not induce cell spreading. For deforming the cell nonspecifically with poly-l-lysine coated beads (n=5; 17.5 Pa stress at 0.3 Hz), there were no significant changes in cell areas ($p>0.70$ and $>0.21$) between 0 and 10 min and between 0 and 20 min, suggesting that stress-induced spreading in mES cells is specific via integrins. Means±s.e. are from at least two independent experiments.

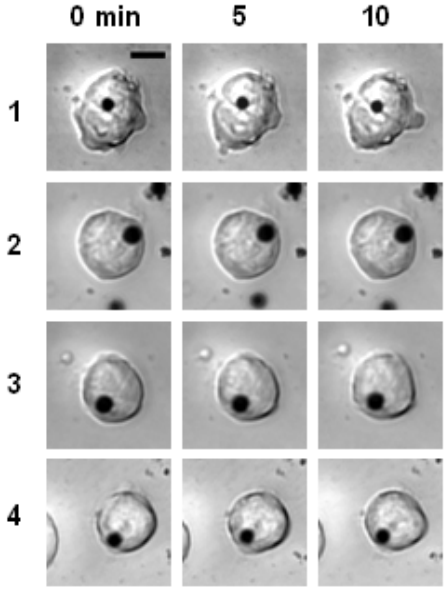


1, Non-target shRNA Control
2, TRCN0000071684: CCGGCTGTCCAAAGACTCCTTTCTTCTCGAGAAGAAAGGAGTCTTTGGACAGTTTTTG
3, TRCN0000071686: CCGGCCGCTAAGTTATCCACAGACACTCGAGTGTCTGTGGATAACTTAGCGGTTTTTG
4, TRCN0000071683: CCGGCGGAATATGTACCAACTGTTTCTCGAGAAACAGTTGGTACATATTCCGTTTTTG

**Fig. S8.** Knocking out Cdc42 blocks stress-induced spreading in mES cells. Procedures were described in Materials and Methods. Corresponding sequences of shRNA for Cdc42 were shown: Lane 1, non-target shRNA control; Lane 2-4, different constructs to knockdown Cdc42. It appears that knockdown of Cdc42 shRNA in Lane 2-4 completely prevented stress-induced spreading. (Scale bar, 10 μm.)

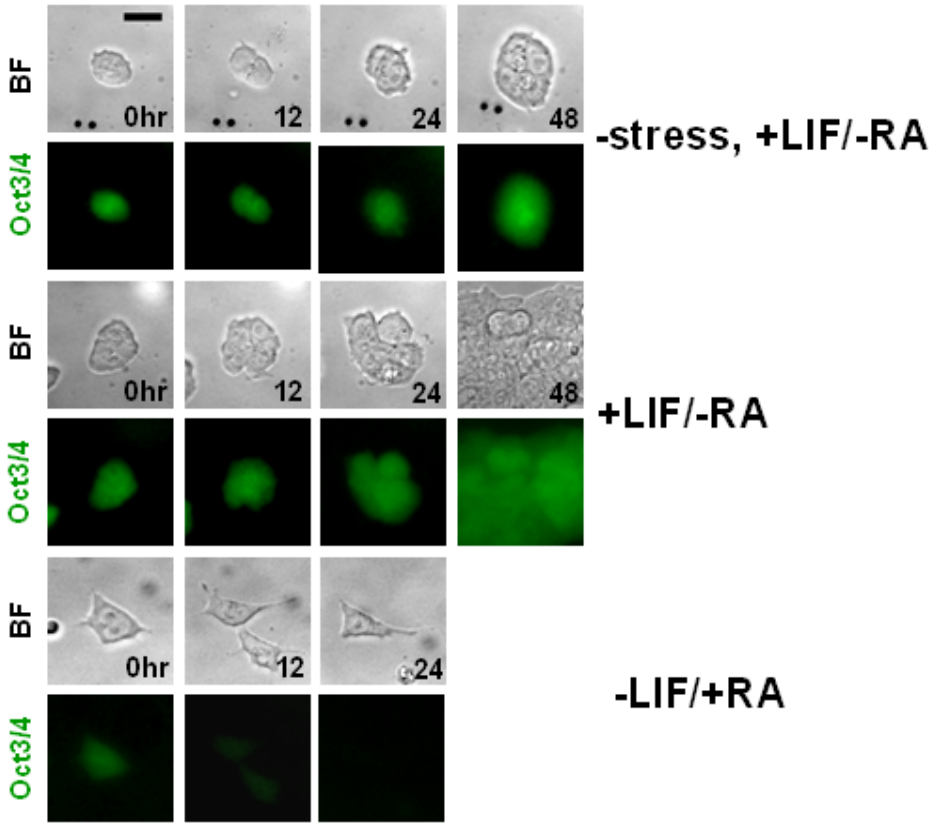


**Fig. S9.** Representative fluorescent images of *Oct3/4* expression under three different conditions. Top: –stress, +LIF/-RA, the cell was in the same dish as +stress, +LIF/-RA condition. Middle: +LIF/-RA, the cell was in a different dish. Bottom: –LIF/+RA, the cell was in the differentiation medium. *Oct3/4* expression increased over time for –stress, +LIF/-RA and +LIF/-RA conditions, whereas it drastically decreased for –LIF/+RA condition. Down-regulation of *Oct3/4* by RA was quick because of a retinoic acid receptor binding domain in the regulatory region of *Oct3/4*. (Scale bar, 10 μm.)

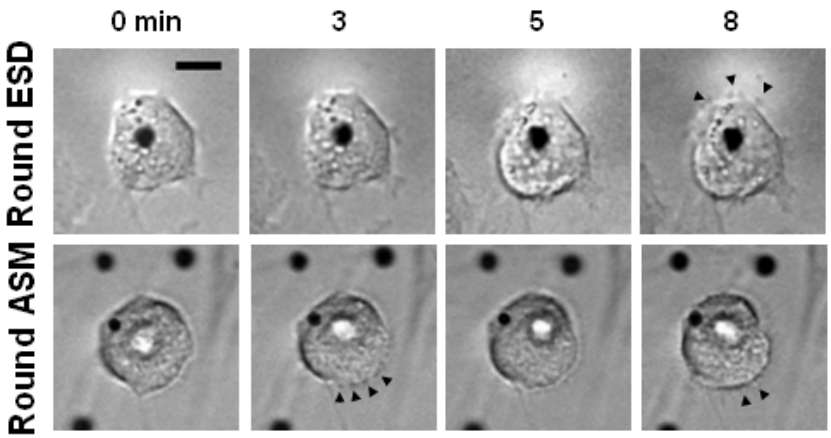


**Fig. S10.** A representative round ESD cell or round ASM cell, plated on low concentration of type I collagen (1 ng/ml), exhibits stress-induced protrusion and spreading (arrowheads), similar to an mES cell. (Scale bar, 10 μm.)

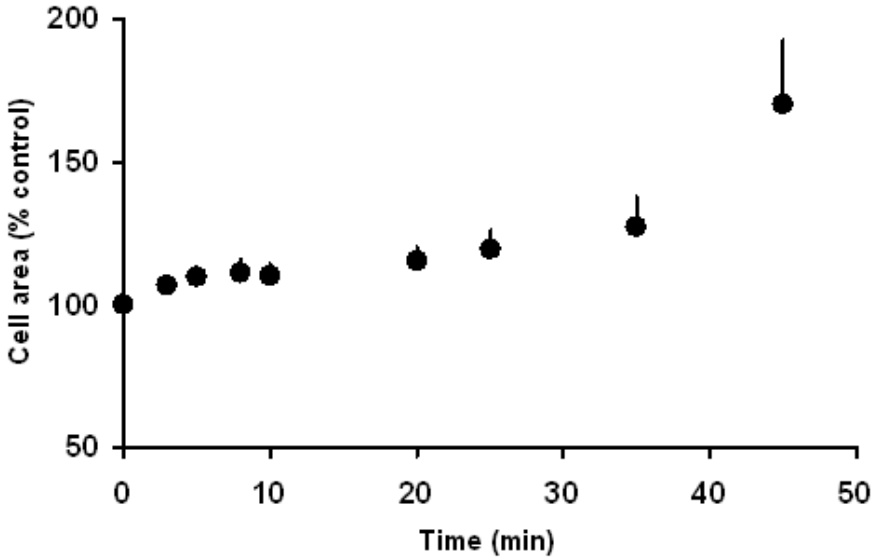


**Fig. S11.** Stress-induced spreading of mES cells at different times. A local cyclic stress (17.5 Pa at 0.3 Hz) was applied for different durations up to 45 min. Cell areas increase by ~ 65% at 45 min. n=9 for each data point, up to 8 min; n=5 from 10 min to 45 min. Mean±s.e. are from at least 3 independent experiments.

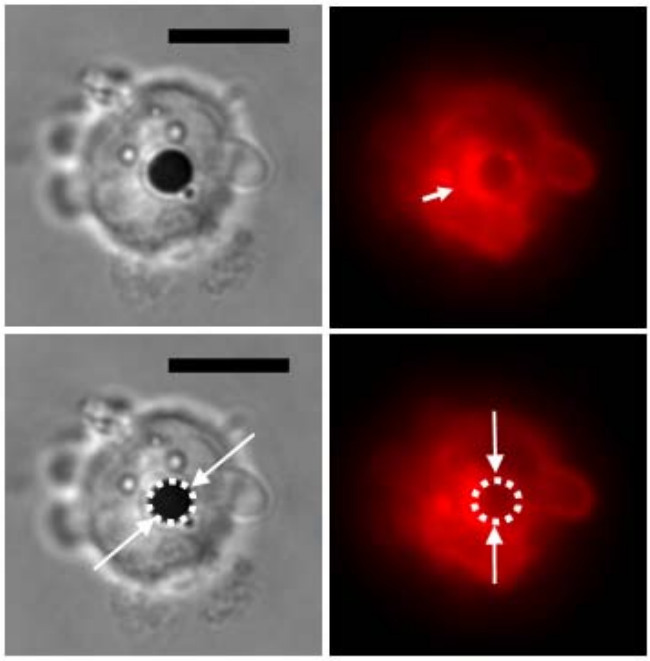

**Fig. S12.** Quantification of magnetic bead embedment in mES cells. An RGD-coated magnetic bead was bound to the apical surface of the mES cell for 15 min. Then the cell was fixed and stained with rhodamine-phalloidin. The recruitment of actin surrounding the bead (small white arrow) was due to the formation of an integrin-mediated focal adhesion at the bead-cell surface contact. By measuring the maximum actin ring diameter from the fluorescent image and the maximum bead diameter from the brightfield image (large white arrows), one can estimate the bead embedment in the cell. This representative cell shows ~50% embedment of the bead. (Scale bar, 15 μm.)

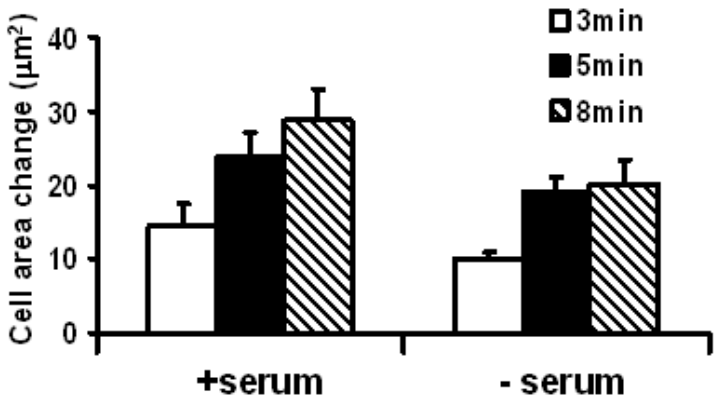


**Fig. S13**. Stress-induced spreading in mES cells occurs in the absence of serum. Compared with the mES cells cultured in 1% serum, mES cells cultured in zero serum also responded to a local cyclic stress (17.5 Pa at 0.3 Hz), although the extent of spreading was somewhat less, especially at longer times (8 min). n= 9 and 8 for 1% serum and no serum condition respectively. There were no significant differences in cell area change between 1% serum and no serum for 3, 5 and 8 min ($p>0.05$). Mean±s.e. Two separate experiments.

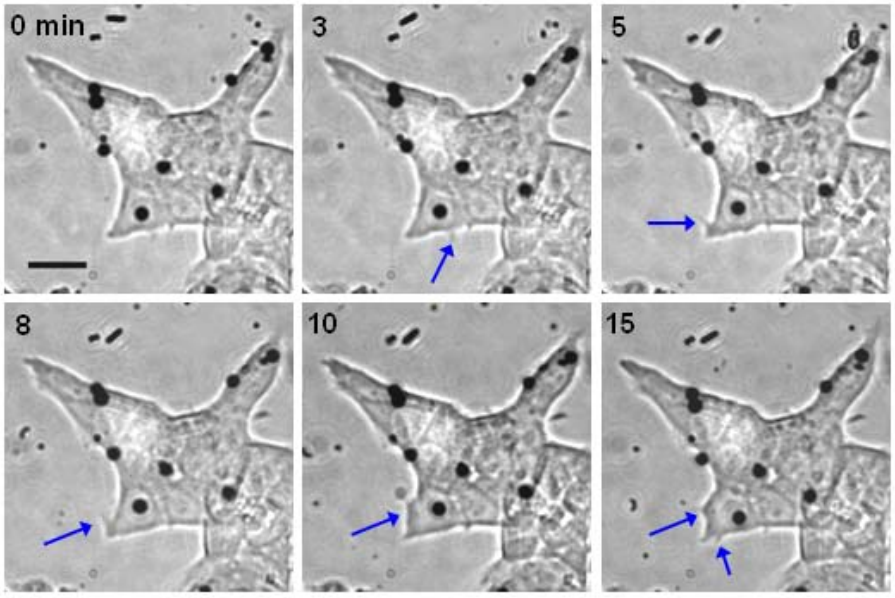


**Fig. S14**. mES cells in a colony also spread in response to a local cyclic stress (17.5 Pa at 0.3 Hz) via a RGD-coated magnetic bead. Blue arrows point to the sites of cell protrusion. Black dots are RGD-coated magnetic beads. The cell area increased significantly after 10-15 min of stress application. (Scale bar, 20 μm.)